NUCL SCI TECH (2019) 30:115
https://doi.org/10.1007/s41365-019-0632-0

Effects of energy deposition on mechanical properties of sodium borosilicate glass irradiated by three heavy ions: P, Kr, and Xe

Xin Du[1] · Tian-Tian Wang[1] · Bing-Huang Duan[1] · Xiao-Yang Zhang[1] · Feng-Fei Liu[1] · Chang-Lin Lan[1] · Guang-Fu Wang[2] · Liang Chen[1] · Hai-Bo Peng[1] · Tie-Shan Wang[1]

Received: 21 September 2018 / Revised: 20 March 2019 / Accepted: 31 March 2019 / Published online: 12 June 2019

Abstract Sodium borosilicate glasses are candidate materials for high-level radioactive waste vitrification; therefore, understanding the irradiation effects in model borosilicate glass is crucial. Effects of electronic energy deposition and nuclear energy deposition induced by the impact of heavy ions on the hardness and Young's modulus of sodium borosilicate glass were investigated. The work concentrates on sodium borosilicate glasses, henceforth termed NBS1 (60.0% SiO_2, 15.0% B_2O_3, and 25.0% Na_2O in mol%). The NBS1 glasses were irradiated by P, Kr, and Xe ions with 0.3 MeV, 4 MeV, and 5 MeV, respectively. The hardness and Young's modulus of ion-irradiated NBS1 glasses were measured by nanoindentation tests. The relationships between the evolution of the hardness, the change in the Young's modulus of the NBS1 glasses, and the energy deposition were investigated. With the increase in the nuclear energy deposition, both the hardness and Young's modulus of NBS1 glasses dropped exponentially and then saturated. Regardless of the ion species, the nuclear energy depositions required for the saturation of hardness and Young's modulus were apparent at approximately 1.2×10^{20} keV/cm^3 and 1.8×10^{20} keV/cm^3, respectively. The dose dependency of the hardness and Young's modulus of NBS1 glasses was consistent with previous studies by Peuget et al. Moreover, the electronic energy loss is less than 4 keV/nm, and the electronic energy deposition is less than 3.0×10^{22} keV/cm^3 in this work. Therefore, the evolution of hardness and Young's modulus could have been primarily induced by nuclear energy deposition.

Keywords Borosilicate glass · Hardness · Young's modulus · Irradiation · Nuclear energy deposition

1 Introduction

Borosilicate glass, which is primarily composed of silicon dioxide and boron trioxide, has been extensively applied to the vitrification of HLW (high-level radioactive waste) [1–5]. Because of the actinide contained in the HLW, alpha particles and recoil nuclei significantly influence the mechanical properties of the glass due to self-irradiation. Therefore, the investigation of variation in the mechanical properties of borosilicate glass after irradiation is significant for the security of long-term geological repository disposal [3, 6–9].

The variations in the mechanical properties of borosilicate glasses with irradiation doses have been studied experimentally [7, 10–13]. Weber et al. presented the results of the hardness evolution of glasses doped with ^{238}Pu where a decrease of approximately 16% in hardness was observed [11]. The authors observed that a decrease in

This work was supported by the National Natural Science Foundations of China (Nos. 11505085 and 11505086), the Fundamental Research Funds for the Central Universities (No. lzujbky-2018-72), and DSTI Foundation of Gansu (No. 2018ZX-07).

✉ Hai-Bo Peng
penghb@lzu.edu.cn

✉ Tie-Shan Wang
tswang@lzu.edu.cn

[1] School of Nuclear Science and Technology, Lanzhou University, Lanzhou 730000, China

[2] Key Laboratory of Beam Technology and Material Modification of Ministry of Education, Beijing Normal University, Beijing 100875, China

hardness of sodium borosilicate glass irradiated by 500 keV helium ions was approximately 14% and the hardness variation saturated when nuclear energy deposition reached approximately 5×10^{20} keV/cm^3 (the nuclear energy deposition value when hardness variation saturated, also known as the saturated nuclear energy deposition) [14]. The variation in the mechanical properties of ^{244}Cm-doped SON68 glass and R7T7 glass with different external heavy-ion irradiations was analyzed by Peuget et al.; they discovered that the hardness of R7T7 and SON68 glass decreased by approximately 35% after heavy-ion irradiation (saturated nuclear energy deposition is 3×10^{20} keV/cm^3) [7, 13, 15]. Peuget et al. suggested that the electronic energy deposition had no effects on hardness variation within 3×10^{22} keV/cm^3 for heavy-ion-irradiated R7T7 glass; thus, the nuclear energy deposition was responsible for changes in the mechanical properties of glasses with heavy-ion irradiation. Recently, Mir et al. proposed that at high electronic energy loss values ($E_e > 4$ keV/nm), the effect of the high electronic energy loss is similar to that of nuclear energy loss. At low electronic energy loss values ($E_e < 1$ keV/nm), electronic collisions could induce some mechanical property changes; however, the magnitude of these changes are lower than those caused by nuclear energy loss [16]. The mechanism of hardness variations induced by irradiation remains unclear, especially after considering the effects of electronic and nuclear processes. Moreover, very few studies have considered the changes of the Young's modulus and the relationships between hardness/modulus, and nuclear energy deposition. Furthermore, the topic of saturated nuclear energy deposition lacks systematic studies. Because the variations in the hardness and Young's modulus versus electronic and nuclear deposition follow an exponential law, the study of saturated nuclear energy deposition has important research significance.

To study the mechanism of variation in the Young's modulus and the hardness on borosilicate glass with heavy-ion irradiation, this work takes a type of sodium borosilicate glass as the object of study, henceforth called NBS1. NBS1 glass samples were irradiated by P, Kr, and Xe ions with energies of 0.3 MeV, 4 MeV, and 5 MeV, respectively. For each of the samples exposed to different irradiation fluences, hardness and Young's modulus were measured by the nanoindentation technique. In addition, the dependence of the hardness variation on the electronic and nuclear energy deposition was studied.

2 Experiments

2.1 Sample preparation

NBS1 glass with the composition of 58.2% SiO_2, 16.8% B_2O_3, and 25.0% Na_2O in mass percent (60.0% SiO_2, 15.0% B_2O_3, and 25.0% Na_2O in mole percentage, K is 4.00, and R is 1.67) was used in this study. The density of NBS1 glass is 2.36 g/cm^3. The Poisson's ratio of NBS1 glass is 0.22. During the elaboration process, silica (SiO_2), orthoboric acid (H_3BO_3), and sodium carbonate (Na_2CO_3) powders were prepared. Platinum/gold (Pt/Au) crucibles were used to retain powder in the elaboration process. The formation of the glass melt undergoes three steps. As an initial step, the decarbonation of Na_2CO_3 was carried out at 800 °C for 4 h to avoid bubble (CO_2) formation, and the dehydration of the orthoboric acid occurred. Next, the glass powder was melted by heating it at 1200 °C for 5 h in atmosphere. Meanwhile, the vitreous liquid was sufficiently stirred. Subsequently, the glass bulk was annealed at 500 °C for 24 h to release inner stress. The size of the NBS1 glass samples is $1 \times 1 \times 0.1$ cm^3. Each sample was polished on both sides to ensure that the roughness of the surface of each glass sample is less than 10 nm. The samples were ultrasonically cleaned in ethanol for 10 min and then dried in air.

2.2 Irradiation experiment

NBS1 glass samples were irradiated by heavy ions as follows: Eight of the samples were irradiated by P ions, seven of the samples were irradiated by Kr ions, and eight of the samples were irradiated by Xe ions; each sample corresponds to a single dose of radiation. The samples for Kr and Xe irradiation were mounted onto a quadrangular prism target holder and then irradiated at 25 °C. One group of the glass samples was irradiated with 4 MeV Kr ions, and the other group was irradiated by 5 MeV Xe ions. The Kr and Xe ions were generated by the 320-kV High-Voltage Platform equipped with an Electron Cyclotron Resonance (ECR) ion source at The Institute of Modern Physics of CAS, Lanzhou [17]. The ion beam was scanned along the X and Y dimensions to irradiate the samples homogeneously. The actual beam spot size used while scanning is 20×20 mm^2. The scanning frequency is 1000 Hz. The flux is 10^{11} ions cm^{-2} s^{-1}. The pressure in the target chamber is 7×10^{-6} Pa. The third group of samples was irradiated with 0.3 MeV P ions at 25 °C that were generated by the accelerator at the Key Laboratory of Beam Technology and Material Modification of the Ministry of Education in Beijing Normal University.

Table 1 Fluences and the corresponding electronic/nuclear energy deposition and the hardness and Young's modulus with different ion irradiation conditions

	Fluence (ions/cm^2)	Electronic energy deposition (keV/cm^3)	Nuclear energy deposition (keV/cm^3)	Hardness (GPa)	Young's modulus (GPa)
Pristine				7.6 ± 0.4	84.9 ± 2.9
300 keV P ions	4.0×10^{11}	1.4×10^{18}	1.4×10^{18}	6.2 ± 0.7	79.6 ± 5.3
	1.4×10^{12}	4.8×10^{18}	5.0×10^{18}	6.2 ± 0.5	80.7 ± 2.4
	4.0×10^{12}	1.4×10^{19}	1.4×10^{19}	6.4 ± 0.6	83.1 ± 4.8
	8.0×10^{12}	2.7×10^{19}	2.9×10^{19}	5.7 ± 0.8	78.3 ± 6.2
	1.4×10^{13}	4.8×10^{19}	5.0×10^{19}	5.5 ± 0.4	77.5 ± 5.3
	4.0×10^{13}	1.4×10^{20}	1.4×10^{20}	4.4 ± 0.4	72.0 ± 3.8
	1.4×10^{14}	4.8×10^{20}	5.0×10^{20}	4.7 ± 0.3	73.4 ± 1.5
	7.0×10^{14}	2.4×10^{21}	2.5×10^{21}	4.5 ± 0.3	71.4 ± 2.0
4 MeV Kr ions	3.0×10^{11}	3.0×10^{18}	2.0×10^{18}	7.5 ± 0.3	85.0 ± 2.5
	3.0×10^{12}	3.0×10^{19}	2.0×10^{19}	6.4 ± 0.2	80.0 ± 2.1
	6.0×10^{12}	6.0×10^{19}	4.0×10^{19}	5.7 ± 0.2	77.1 ± 1.8
	1.0×10^{13}	9.9×10^{19}	6.7×10^{19}	5.4 ± 0.3	76.3 ± 3.0
	3.0×10^{13}	3.0×10^{20}	2.0×10^{20}	4.9 ± 0.2	71.9 ± 2.1
	1.0×10^{14}	9.9×10^{20}	6.7×10^{20}	4.8 ± 0.2	69.3 ± 1.9
	5.0×10^{14}	4.9×10^{21}	3.3×10^{21}	4.8 ± 0.2	69.2 ± 1.7
5 MeV Xe ions	6.1×10^{11}	7.6×10^{18}	7.9×10^{18}	6.5 ± 0.5	81.1 ± 3.6
	1.8×10^{12}	2.2×10^{19}	2.3×10^{19}	6.0 ± 0.3	80.4 ± 1.8
	3.6×10^{12}	4.5×10^{19}	4.7×10^{19}	5.3 ± 0.4	75.5 ± 2.8
	6.1×10^{12}	7.6×10^{19}	7.9×10^{19}	4.7 ± 0.2	70.9 ± 1.3
	1.8×10^{13}	2.2×10^{20}	2.3×10^{20}	4.4 ± 0.2	68.4 ± 1.9
	6.1×10^{13}	7.6×10^{20}	7.9×10^{20}	4.5 ± 0.2	69.1 ± 1.5
	3.0×10^{14}	3.7×10^{21}	3.9×10^{21}	4.6 ± 0.2	68.7 ± 1.6
	6.1×10^{14}	7.6×10^{21}	7.9×10^{21}	4.5 ± 0.2	66.1 ± 1.5

Table 1 shows the fluences and electronic and nuclear energy deposition for each of the irradiated samples. The projected penetration depths of P, Kr, and Xe ions in NBS1 glass are approximately 0.4, 2.4, and 1.97 μm, respectively, that were calculated using the SRIM (version-2008) code [18, 19].

Figure 1 shows the nuclear, electronic, and total energy losses of the P, Kr, and Xe ions in NBS1 glass. The energy loss was obtained by the SRIM program. The dashed, dotted, and solid lines represent the electronic, nuclear, and total energy loss in NBS1 glass, respectively.

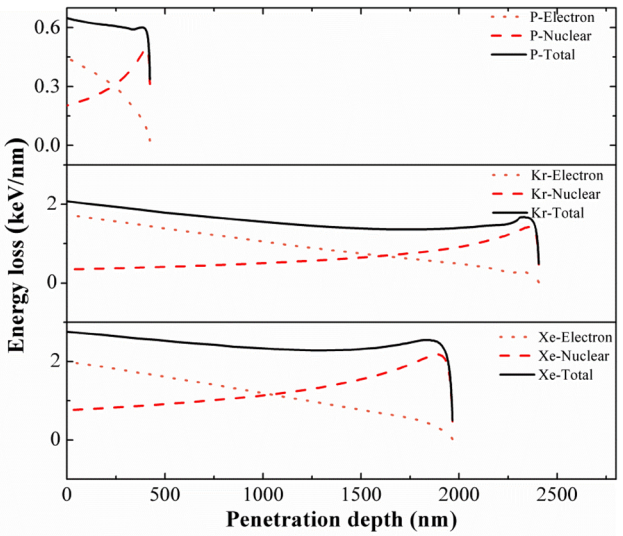

Fig. 1 (Color online) The electronic, nuclear, and total energy loss of P ions, Kr ions, and Xe ions in NBS1 glass

2.3 Measurements of Hardness and Young's Modulus

The hardness and Young's modulus of the NBS1 glasses were obtained by an MTS G200 Nanoindenter with a Berkovich diamond indenter [20]. Nanoindentation tests were performed in continuous stiffness measurement (CSM) mode at 25 °C. The maximum penetrating depth of the indenter went up to 2 μm, and the maximum load was

500 mN. The measured hardness of fused silica was used to calibrate the MTS G200 device before the measurement of the hardness of the NBS1 glass samples, and the system error was obtained through the corresponding measurements of fused silica.

The details of the nanohardness measurement were introduced by Oliver [21, 22]. The nanohardness is defined by Eq. (1):

$$H = \frac{P_s}{A}, \tag{1}$$

where H is the hardness of the NBS1 glass, P_s is the load on the indenter, and A is the projected area of the hardness impression after unloading.

The stiffness of glass follows Eq. (2):

$$S = \beta \frac{2}{\sqrt{\pi}} E_{\text{eff}} \sqrt{A}, \tag{2}$$

where E_{eff} is the reduced modulus and β implies that the nanoindenter has a constant geometry.

The E_{eff} can be defined as:

$$\frac{1}{E_{\text{eff}}} = \frac{1-v^2}{E} + \frac{1-v_i^2}{E_i}, \tag{3}$$

where E and v are the Young's modulus and Poisson's ratio of NBS1 glass, respectively, and E_i and v_i of the indenter are 1141 GPa and 0.07 GPa, respectively [21, 22]. The value of ν is set 0.22. Therefore, according to Eqs. (1)–(3), the relationship between the hardness and the Young's modulus can be expressed as:

$$H = \frac{4}{\pi} \beta^2 \left(\frac{E}{0.95} \right) \frac{P_s}{S^2}. \tag{4}$$

3 Results

The measured Young's modulus and hardness curves of pristine samples of NBS1 glass, versus those from P-, Kr-, and Xe-ion-irradiated NBS1 glasses, are presented in Figs. 2 and 3. The solid lines show the measured values of the hardness and the Young's modulus of the pristine NBS1 glasses. As shown in Fig. 2, the dashed and dash-dot lines are the hardness measuring curves of Kr- and Xe-ion-irradiated NBS1 glasses, respectively, and the dotted and short dotted lines are the Young's modulus measuring curves of the Kr- and Xe-ion-irradiated NBS1 glasses. The short-dashed line and short dash-dot line in Fig. 3 are the hardness and Young's modulus measuring curves of NBS1 glasses irradiated by P ions. The curves fluctuate significantly at the surface because of the blunt tip of the indenter and surface effects. However, the measurement curves of pristine NBS1 glass were almost flat with a penetration depth from 200 to 2000 nm, indicating that the nanohardness of the pristine glass was independent of the depth. The hardness and Young's modulus curves of Kr- and Xe-ion-irradiated NBS1 glasses were not flat until a penetration depth of 1400 nm. For P-ion-irradiated NBS1 glasses, the curves were not flat until a penetration depth of 400 nm, and the irradiated zone was 400 nm.

Peuget et al. proposed that the plastic interaction zone appeared to extend to approximately twice the penetration depth, and that the Young's modulus and hardness obtained at half of the depth that ions penetrated represent the response of the irradiated zone [7, 10, 15]. Therefore, the Young's modulus and hardness obtained at depths in the range of 0–1000 nm (here, we select the region between 300 and 800 nm) should reflect the response of the irradiated zone in Kr- and Xe-ion-irradiated NBS1 glasses. Next, the Young's modulus and hardness obtained at depths in the range 0–200 nm (here, we select the region between 100 and 200 nm) should reflect the response of the irradiated zone in P-ion-irradiated NBS1 glasses. Extrapolation methods were used to obtain the hardness and Young's modulus values in this work. Peng et al. compared three different methods to obtain the hardness values with CSM, and they suggested that the extrapolation method could be used to compare the results with different ion ranges [23, 24]. Therefore, the hardness of glass was obtained by extrapolating data with penetrated depth from 300 to 800 nm for Kr- and Xe-ions-irradiated NBS1 glasses, and from 100 to 200 nm for P-ions-irradiated NBS1 glasses. The same situation was set up to obtain the value of Young's modulus.

To analyze the hardness evolution in NBS1 glasses irradiated with heavy ions, the relative variation in hardness was introduced, and the relative variation in hardness of ^{244}Cm-doped SON68 in the work of Peuget et al. [7, 10, 15] was compared with the hardness variation in the NBS1 glasses. The relative variation in hardness of NBS1 glasses and the data of Peuget et al. are shown in Figs. 4 and 5. The symbols with error bars present the relative variation in hardness and Young's modulus of NBS1 glass with heavy-ion irradiation, and the open symbols without error bars represent the relative variation in hardness of Cm-doped SON68 glass. As shown in Figs. 4 and 6, the relative variation in hardness and the Young's modulus of irradiated NBS1 glass dropped with increasing nuclear energy deposition. When nuclear energy deposition reached approximately 1.2×10^{20} keV/cm^3, the hardness variation saturated, in agreement with previous studies [3, 7, 10, 11, 13–15, 23, 25, 26]. Moreover, the hardness variation of Cm-doped SON68 glasses also stabilized above 3.0×10^{20} keV/cm^3. Note that the transformation region was also identical for different types of heavy ions.

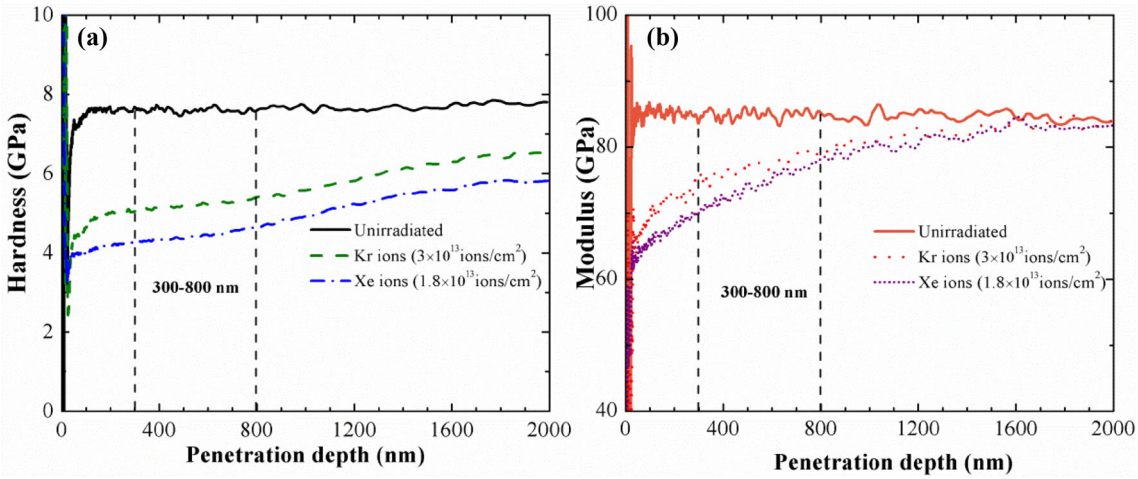

Fig. 2 (Color online) Evolution of the hardness (**a**) and modulus (**b**) (0–2000 nm) of pristine NBS1 glass and Kr- and Xe-ions-irradiated NBS1 glass (The penetration depths of indenter were 2 μm, and the maximum load is 500 mN)

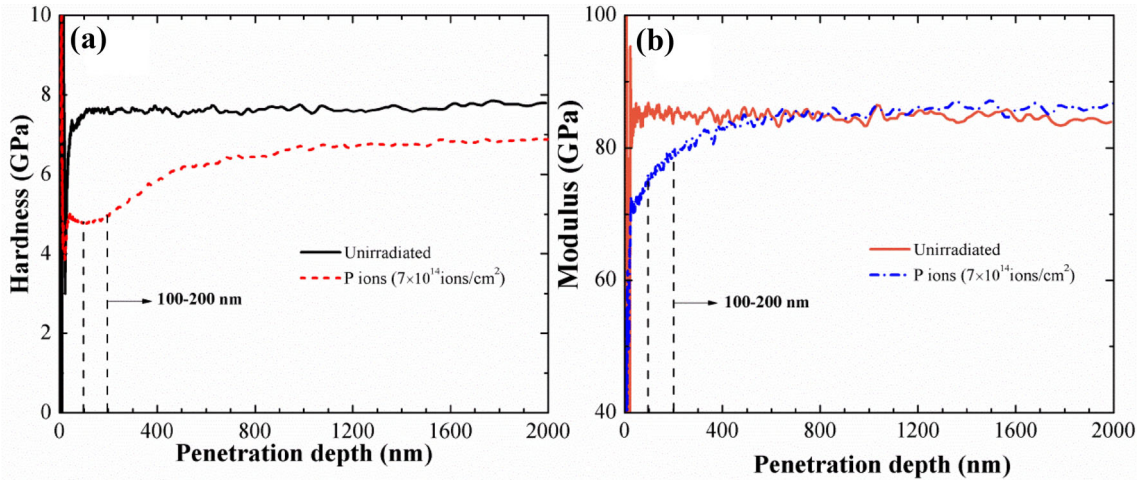

Fig. 3 (Color online) Evolution of the hardness (**a**) and modulus (**b**) (0–2000 nm) of pristine NBS1 glass and P-ion-irradiated NBS1 glass (The penetration depths of the indenter were 2 μm, and maximum load is 500 mN)

The transformation region of nuclear energy deposition ranged from 4.8×10^{19} to 1.2×10^{20} keV/cm^3.

DeNatale et al. proposed the following calculation formulas for the energy deposition in silicate glasses with ion irradiation [27]:

$$E_{\text{nucl}} = E_{\text{ion}} \cdot \frac{S_{\text{n}}}{S_{\text{n}} + S_{\text{e}}} \cdot \frac{\Phi}{R}, \tag{5}$$

$$E_{\text{elec}} = E_{\text{ion}} \cdot \frac{S_{\text{e}}}{S_{\text{n}} + S_{\text{e}}} \cdot \frac{\Phi}{R}, \tag{6}$$

where E_{nucl} is the nuclear energy deposition, E_{elec} is the electronic energy deposition, Φ is the fluence in ions/cm^2, R is the projectile depth of heavy ions in the glass that is calculated by the SRIM (version-2008) program [18], and E_{ion} is the incidental energy. Moreover, S_{n} and S_{e} are the average nuclear and electronic energy losses, respectively.

4 Discussion

4.1 Hardness

For the NBS1 glasses irradiated with P, Kr, and Xe ions, the hardness decreased with the energy deposition. Although the ion species are different, the maximum decreases in relative variation in hardness are all approximately 36% for NBS1 glasses. The decreasing trend of hardness variation obeys Eq. (7):

$$\frac{\Delta H}{H} = V_H\left(1 - e^{-\frac{\text{dose}}{t_{\text{H}}}}\right), \tag{7}$$

where H is the hardness of NBS1 glass, ΔH is the variation in hardness (the difference between the hardness of irradiated NBS1 glass and that of pristine NBS1 glass), V_{H} corresponds to the maximum value of the relative variation

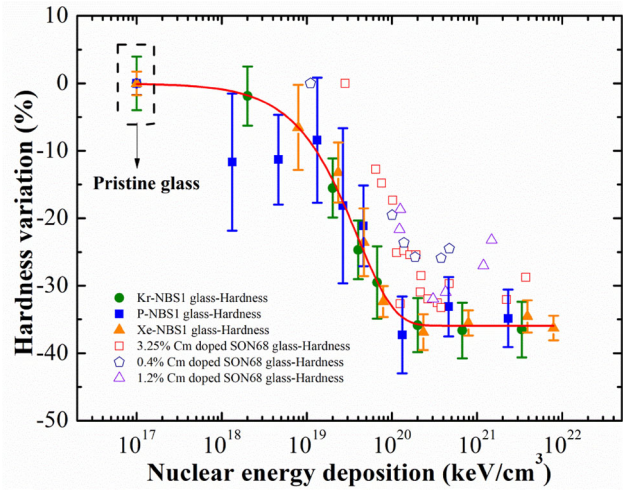

Fig. 4 (Color online) Relative variation of hardness versus nuclear energy deposition (keV/cm^3) in NBS1 and Cm-doped SON68 glasses

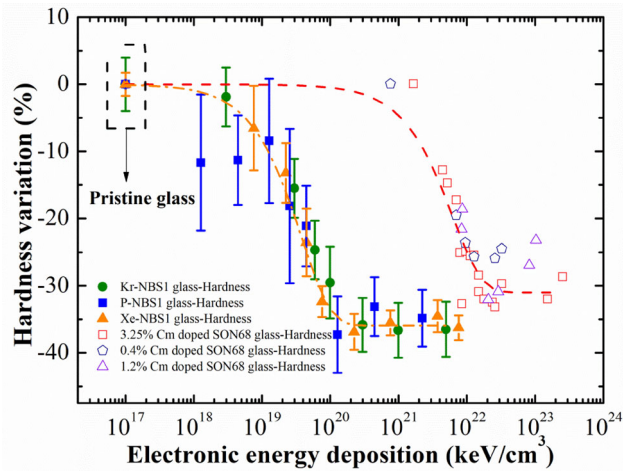

Fig. 5 (Color online) Relative variation of hardness versus electronic energy deposition (keV/cm^3) in NBS1 and Cm-doped SON68 glasses

in hardness, and t_H is the decay constant for the relative variation in hardness. The decreased hardness of borosilicate glasses impacted by heavy ions has been widely studied. In Karakurt's study, the relative variation in hardness of borosilicate glasses impacted with Au ions was approximately 38% [12]. A series of CJ glasses were studied by Bonfils et al. [25]. The maximum decrease in the relative variation in the hardness of a glass sample with multi-energy gold ion irradiation was approximately 35%. The hardness variation of SON68 glass doped with ^{244}Cm and ^{238}Pu was 25% in the study of Inagaki et al. [28]. The dependency of the decrease in hardness on the dose expressed by Eq. (7) is also in agreement with the results by Peuget and Weber [7, 10, 11, 13, 15]. In the study of Abbas et al., a decrease of 20% in the hardness of aluminoborosilicate glasses was observed [29]. In the aforementioned works, the maximum decreases in the hardness

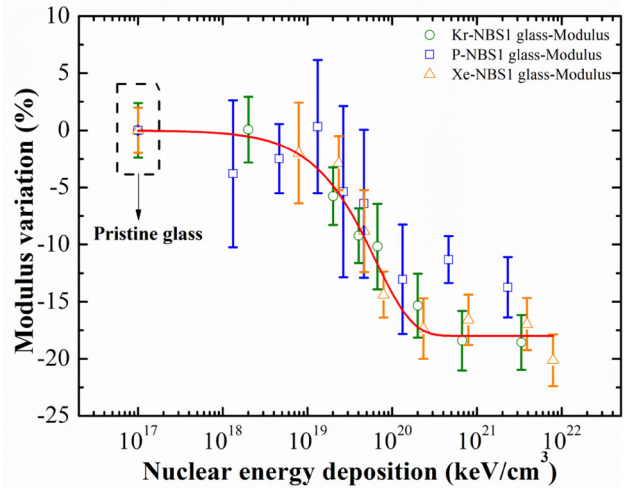

Fig. 6 (Color online) Relative variation of modulus versus nuclear energy deposition (keV/cm^3) in NBS1 glass

variation were approximately 35% or 25% in borosilicate glasses with ion irradiation. This difference in the value of hardness variation can be attributed to the difference in the chemical composition of the glasses. The hardness variation, induced by irradiation of ions, was correlated with changes in the microstructures of glasses. Indeed, the ion irradiation induced modifications in the glass network, such as non-bridge oxygen [30], transformation of [BO_4] to [BO_3] units [31, 32], and ring structure [33], which could lead to hardness variation. Changes in the sodium composition of the glasses also led to transformations of [BO_4] to [BO_3] units. Some other actions, such as action by calcium, might play a similar role in glass as that played by sodium. However, the manner in which the composition of glass influences its hardness variation when it is irradiated by ions is still unknown.

During the irradiation of NBS1 glasses with heavy ions, two processes of energy deposition were generated: (1) inelastic collision, which involves collision of projectile ions with electrons of material atoms, and (2) elastic scattering, which involves a collision of projectile ions with material atoms [34]. The processes of inelastic collisions and elastic scattering correspond to electronic and nuclear energy deposition in glass impacted by heavy ions, respectively.

The hardness evolution of Cm-doped SON68 glass and R7T7 glass irradiated with heavy ions was directly compared in the study of Peuget et al. [7, 13, 15]. The hardness variations of Cm-doped SON68 and R7T7 glasses show very good agreement with the nuclear energy deposition. However, the hardness variations with the electronic energy deposition were inconclusive. Therefore, Peuget et al. suggested that hardness variations were caused by the nuclear process. To study the effects of electronic and

nuclear processes in sodium borosilicate glass, the hardness values of Cm-doped SON68 glasses were introduced in this work. Figures 4 and 5 show the relative variations in hardness of NBS1 and Cm-doped SON68 glasses. A comparison of the hardness variations of NBS1 and Cm-doped SON68 glasses with those due to nuclear energy deposition is shown in Fig. 4. Good agreement in the hardness variation values and similar evolutionary trends were observed; the saturated nuclear energy deposition of relative variation in hardness of NBS1 glasses is close to that in Cm-doped SON68 glasses. However, the saturated electronic energy deposition in Cm-doped SON68 glasses was 2.0×10^{22} keV/cm^3 and was far above that in NBS1 glasses shown in Fig. 5. Therefore, the hardness variation in heavy-ion-irradiated NBS1 glasses can be mainly attributed to nuclear interactions.

Many researchers have studied the hardness variations in glasses. In Mir et al.'s work, BS3 and SON68 glasses were irradiated by heavy-ion beams [16]. They found that a significant modification of glasses was caused by nuclear energy loss and high electronic energy loss when the electronic energy loss was greater than 4 keV/nm. In this study, the electronic energy loss was approximately 2.00, 1.75, and 0.45 keV/nm for Xe-, Kr-, and P-ions-irradiated NBS1 glass, respectively; the values are all less than 4 keV/nm. As shown in Table 1, the maximum electron energy depositions were all less than 3.0×10^{22} keV/cm^3. (The nuclear energy deposition was mainly responsible for the variations in the hardness of glasses with heavy-ion irradiation when the electronic energy deposition was less than 3×10^{22} keV/cm^3 in the study of Peuget et al. [7, 13, 15].) The hardness of the electron-irradiated sodium borosilicate glasses was found to decrease approximately by only 4% [14]; therefore, Yang et al. considered the nuclear energy deposition to be the primary factor in the evolution of hardness in borosilicate glass. The alpha particles irradiation was found to induce evolution of the glass hardness in the studies of Weber and Matzke, and they also indicated that the decrease in hardness was induced by nuclear energy deposition [11]. The hardness variation with the nuclear energy deposition showed good agreement with previous studies [7, 10, 15], indicating that it was primarily caused by the nuclear energy deposition effect.

The saturated nuclear energy deposition of the hardness was proposed in different works. For example, the hardness variation stabilized with the nuclear energy deposition of 5.5×10^{20} keV/cm^3 in sodium borosilicate glass [3]. The saturated nuclear energy deposition was approximately 3.0×10^{20} keV/cm^3 in SON68 and R7T7 glass [7, 10, 15]. Peng et al. proposed that when the displacement per atom (dpa) reached 0.02 (2.0×10^{20} keV/cm^3 of nuclear energy deposition) [23], the hardness variation stabilized. The saturated nuclear energy deposition of the hardness is 1×10^{20} keV/cm^3 in ISG glass irradiated with helium ions [12]. In addition, there was no systematic research regarding the saturated nuclear energy deposition in borosilicate glasses with heavy-ion irradiation before this work. The saturated nuclear energy deposition in numerous research studies is similar, being within the same order of magnitude as shown in Table 2. The small difference in saturated nuclear energy deposition is possibly caused by the composition of the glasses.

4.2 Young's modulus

Although the ion species are different, the maximum decreases in the Young's modulus are approximately 17.9% for NBS1 glasses. The decreasing trend of the Young's modulus variation obeys Eq. (8):

$$\frac{\Delta E}{E} = V_{\mathrm{E}}\left(1 - e^{-\frac{\mathrm{dose}}{t_{\mathrm{E}}}}\right), \tag{8}$$

where E is the Young's modulus of NBS1 glass, ΔE represents the changes in the Young's modulus (the difference between the Young's modulus of irradiated NBS1 glass and that of pristine NBS1 glass), V_{E} corresponds to the maximum of the relative variation in Young's modulus, and t_{E} is the decay constant for the relative variation in Young's modulus. In the study of Karakurt et al., the decrease of approximate 3% and 8% was observed in the relative variation in Young's modulus of the SON68 and ISG glass with Au ion irradiation [12], respectively. The relative variation in the modulus of SON68 glass doped with ^{244}Cm was approximately 15% [13]. The relative variation in the modulus of ^{244}Cm-doped glass was presented by Inagaki et al. [28]; the decrease in the modulus was approximately 30%. This difference in the modulus variation could also be caused by differences in the chemical composition of the glasses.

As shown in Fig. 6, the Young's modulus variation decreased with the increasing nuclear energy deposition followed by stabilization, where the nuclear energy deposition is approximately 1.8×10^{20} keV/cm^3. The Young's modulus variation of NBS1 glass with heavy-ion irradiation is in good agreement with the study of Peuget et al., and they proposed that the Young's modulus variation of Cm-doped SON68 glass was induced by nuclear energy deposition [13]. As shown in Figs. 4 and 6, the same variation trend in the hardness and the modulus is observed. The hardness variation stabilized at a nuclear energy deposition of 1.2×10^{20} keV/cm^3. Moreover, the saturated nuclear energy deposition of the relative variation in hardness of NBS1 glasses was close to that of the relative variation in Young's modulus, and their orders of magnitude are the same. The transformation region of

Table 2 The saturated nuclear energy deposition in different studies

Study	Type of glass	$[SiO_2]$ (wt%)	$[B_2O_3]$ (wt%)	$[Na_2O]$ (wt%)	Others (wt%)	Saturated nuclear energy deposition (keV/nm^3)
Peuget et al.	R7T7	45.5	14.0	9.8	30.7	3.0×10^{20}
Zhang et al.	T	70.0	4.0	17.0	9.0	5.5×10^{20}
Yang et al.	T^+	68.0	15.0	9.0	8.0	5.0×10^{20}
Karakurt et al.	ISG	56.2	17.3	12.2	14.3	1.0×10^{20}
This work	NBS1	58.2	16.8	25.0	0.0	1.2×10^{20}

Young's modulus variation was also close to that of the hardness variation. Therefore, it is probable that the variation in Young's modulus is mainly caused by the nuclear energy deposition.

5 Conclusion

Irradiation effects induced by 300 keV P ions, 4 MeV Kr ions, and the 5 MeV Xe ions on borosilicate glass were studied. According to the results, the nuclear energy deposition on the saturation of relative variation in hardness of NBS1 glasses is the same order of magnitude as that of the relative variation in Young's modulus. Furthermore, the transformation region of the Young's modulus variation was found to be close to that of the hardness variation. The variations in Young's modulus and hardness with the nuclear energy deposition showed good agreement with previous studies in the literature. Therefore, we conclude that the evolution of the Young's modulus as well as that of the hardness in the NBS1 glasses is primarily the consequence of nuclear energy deposition.

Acknowledgments The authors are grateful to the staff of the 320-kV ECR HCIs Platform at IMP (Lanzhou), and the staff of the Public Center for Characterization and Test at Suzhou Institute of Nano-tech and Nano-bionics for their technical support.

References

1. D. Manara, A. Grandjean, D.R. Neuville, Structure of borosilicate glasses and melts: a revision of the Yun, Bray and Dell model. J. Non-Cryst. Solids **355**, 2528–2531 (2009). https://doi.org/10.1016/j.jnoncrysol.2009.08.033
2. T.S. Wang, X. Du, W. Yuan et al., Morphological study of borosilicate glass surface irradiated by heavy ions. Surf. Coat. Technol. **306**, 245–250 (2016). https://doi.org/10.1016/j.surfcoat.2016.06.018
3. G.F. Zhang, T.S. Wang, K.J. Yang et al., Raman spectra and nano-indentation of Ar-irradiated borosilicate glass. Nucl. Instrum. Methods B **316**, 218–221 (2013). https://doi.org/10.1016/j.nimb.2013.09.020
4. W.L. Gao, B.X. Xia, Q.X. Xu et al., Immobilization of radioactive fluoride waste in aluminophosphate glass:a molecular dynamics simulation. Nucl. Sci. Tech. **29**, 92 (2018). https://doi.org/10.1007/s41365-018-0443-8
5. Y.P. Sun, X.B. Xia, Y.B. Qiao et al., Properties of phosphate glass waste forms containing fluorides from a molten salt reactor. Nucl. Sci. Tech. **27**, 63 (2016). https://doi.org/10.1007/s41365-016-0059-9
6. G.K. Lockwood, S.H. Garofalini, Effect of moisture on the self-healing of vitreous silica under irradiation. J. Nucl. Mater. **400**, 73–78 (2010). https://doi.org/10.1016/j.jnucmat.2010.02.012
7. S. Peuget, N.J. Cachia, C. Jégou et al., Irradiation stability of R7T7-type borosilicate glass. J. Nucl. Mater. **354**, 1–13 (2006). https://doi.org/10.1016/j.jnucmat.2006.01.021
8. R.A.B. Devine, Macroscopic and microscopic effects of radiation in amorphous SiO_2. Nucl. Instrum. Methods B **91**, 378–390 (1994). https://doi.org/10.1016/0168-583X(94)96253-7
9. B. Boizot, S. Agnello, B. Reynard et al., Raman spectroscopy study of beta-irradiated silica glass. J. Non-Cryst. Solids **325**, 22–28 (2003). https://doi.org/10.1016/S0022-3093(03)00334-X
10. S. Peuget, V. Broudic, C. Jegouu et al., Effect of alpha radiation on the leaching behaviour of nuclear glass. J. Nucl. Mater. **362**, 474–479 (2007). https://doi.org/10.1016/j.jnucmat.2007.01.099
11. W.J. Weber, H.J. Matzke, Indentation fracture toughness in nuclear waste glasses and ceramics: environmental and radiation effects. Euro. Appl. Res. Rep. **7**, 207 (1987)
12. G. Karakurt, A. Abdelouas, J.P. Guin et al., Understanding of the mechanical and structural changes induced by alpha particles and heavy ions in the French simulated nuclear waste glass. J. Nucl. Mater. **2016**(475), 243–254 (2016). https://doi.org/10.1016/j.jnucmat.2016.04.022
13. S. Peuget, J.M. Delaye, C. Jégou, Specific outcomes of the research on the radiation stability of the French nuclear glass towards alpha decay accumulation. J. Nucl. Mater. **444**, 76–91 (2014). https://doi.org/10.1016/j.jnucmat.2013.09.039
14. K.J. Yang, T.S. Wang, G.F. Zhang et al., Study of irradiation damage in borosilicate glass induced by He ions and electrons. Nucl. Instrum. Methods B **307**, 541–544 (2013). https://doi.org/10.1016/j.nimb.2012.12.113
15. S. Peuget, P.Y. Noel, J.L. Loubet et al., Effects of deposited nuclear and electronic energy on the hardness of R7T7-type containment glass. Nucl. Instrum. Methods B **246**, 379–386 (2006). https://doi.org/10.1016/j.nimb.2005.12.053
16. A.H. Mir, I. Monnet, M. Toulemonde et al., Mono and sequential ion irradiation induced damage formation and damage recovery in oxide glasses: stopping power dependence of the mechanical properties. J. Nucl. Mater. **469**, 244–250 (2016). https://doi.org/10.1016/j.jnucmat.2015.12.004
17. Y. Yang, J.Y. Yuan, C.Y. Feng et al., Transmission efficiency improvement of the injector line of SFC by particle beam decorrelation. Nucl. Sci. Tech. **26**, 060203 (2015). https://doi.org/10.13538/j.1001-8042/nst.26.060203

18. J.F. Ziegler, J.P. Biersack, The stopping and range of ions in matter. Nucl. Instrum. Methods B. F, 93–129 (1985). https://doi.org/10.1007/978-1-4615-8103-1_3
19. D. Saad, H. Benkharfia, M. Izerrouken et al., Displacement damage cross section and mechanical properties calculation of an Es-Salam research reactor aluminum vessel. Nucl. Sci. Tech. **28**, 162 (2017). https://doi.org/10.1007/s41365-017-0319-3
20. W. Qi, Z.T. He, B.L. Zang et al., Behaviors of fine(IG-110) and ultra-fine(HPG-510) grain graphite irradiated by 7 MeV Xe^{26+} ions. Nucl. Sci. Tech. **28**, 144 (2017). https://doi.org/10.1007/s41365-017-0292-x
21. W.C. Oliver, G.M. Pharr, An improved technique for determining hardness and elastic modulus using load and displacement sensing indentation experiments. J. Mater. Res. **7**, 1564–1583 (1992). https://doi.org/10.1557/JMR.1992.1564
22. W.C. Oliver, G.M. Pharr, Measurement of hardness and elastic modulus by instrumented indentation: advances in understanding and refinements to methodology. J. Mater. Res. **19**, 3–20 (2004). https://doi.org/10.1557/jmr.2004.19.1.3
23. H.B. Peng, M.L. Sun, X. Du et al., Variation of hardness and modulus of borosilicate glass irradiated with Kr ions. Nucl. Instrum. Methods B **406**, 561–565 (2017). https://doi.org/10.1016/j.nimb.2017.04.057
24. H.B. Peng, F.F. Liu, M. Guan, Variation of hardness and modulus of sodium borosilicate glass irradiated with different ions. Nucl. Instrum. Methods B **435**, 214–218 (2018). https://doi.org/10.1016/j.nimb.2018.01.006
25. J.D. Bonfils, S. Peuget, G. Panczer et al., Effect of chemical composition on borosilicate glass behavior under irradiation. J. Non-Cryst. Solids **356**, 388–393 (2010). https://doi.org/10.1016/j.jnoncrysol.2009.11.030
26. L. Chen, W. Yuan, S. Nan et al., Study of modifications in the mechanical properties of sodium aluminoborosilicate glass induced by heavy ions and electrons. Nucl. Instrum. Methods B **370**, 42–48 (2016). https://doi.org/10.1016/j.nimb.2016.01.007
27. J.F. Denatale, D.G. Howitt, G.W. Aranold, Radiation damage in silicate glass. Radiat. Eff. **98**, 63–70 (1986). https://doi.org/10.1080/00337578608206098
28. Y. Inagaki, H. Furuya, Y. Ono et al., Effects of α-decay on mechanical properties of simulated nuclear waste glass. Mater. Res. Soc. Symp. Proc. **294**, 191–198 (1992). https://doi.org/10.1557/proc-294-191
29. A. Abbas, Y. Serruys, D. Ghaleb et al., Evolution of nuclear glass structure under α-irradiation. Nucl. Instrum. Methods B **166–167**, 445–450 (2000)
30. D.A. Kilymis, J.M. Delaye, Deformation mechanisms during nanoindentation of sodium borosilicate glasses of nuclear interest. J. Chem. Phys. **141**, 014504 (2014). https://doi.org/10.1063/1.4885850
31. C. Mendoza, S. Peuget, T. Charpentier et al., Oxide glass structure evolution under swift heavy ion irradiation. Nucl. Instrum. Methods B **325**, 54–65 (2014). https://doi.org/10.1016/j.nimb.2014.02.002
32. L.H. Kieu, J.M. Delaye, C. Stolz, Modeling the effect of composition and thermal quenching on the fracture behavior of borosilicate glass. J. Non-Cryst. Solids **358**, 3268–3279 (2012). https://doi.org/10.1016/j.jnoncrysol.2012.07.037
33. R. Boffy, S. Peuget, R. Schweins et al., High thermal neutron flux effects on structural and macroscopic properties of alkali-borosilicate glasses used as neutron guide substrate. Nucl. Instrum. Methods B **374**, 14–19 (2016). https://doi.org/10.1016/j.nimb.2015.10.011
34. H.B. Peng, M.L. Sun, K.J. Yang et al., Effect of irradiation on hardness of borosilicate glass. J. Non-Cryst. Solids **443**, 143–147 (2016). https://doi.org/10.1016/j.jnoncrysol.2016.04.027